Image analysis reveals that *Escherichia coli* RecA protein consists of two domains

Xiong Yu and Edward H. Egelman
Department of Molecular Biophysics and Biochemistry, Yale University, New Haven, Connecticut 06511

ABSTRACT The *Escherichia coli* RecA protein catalyzes homologous genetic recombination by forming helical polymers around DNA molecules. These polymers have an ATPase activity, which is essential for the movement of strands between two DNA molecules. One obstacle to structural studies of the RecA filament has been that the ATPase results in a dynamical polymer containing a mixture of states with respect to the bound ATP and its hydrolytic products. We have formed filaments which are trapped in the ADP-P_i state by substituting AlF_4^- for the P_i, and have used these stable filaments to generate a three-dimensional reconstruction from electron micrographs. The resolution of the reconstruction is sufficient to resolve the 38-k RecA subunit into two nearly equal domains. This reconstruction provides the most detailed view yet of the RecA protein, and serves as a framework within which existing biochemical data on RecA can be understood.

INTRODUCTION

The *Escherichia coli* RecA protein is involved in general genetic recombination, DNA repair and phage induction in vivo. This protein has been used in vitro to mediate the search for homology between different DNA molecules and to promote a strand exchange reaction between homologous DNA molecules (for reviews, see Howard-Flanders et al., 1984; Cox and Lehman, 1987).

The activity of the RecA protein can be examined with respect to both the strand exchange reaction (Howard-Flanders et al., 1984) and the cleavage of the LexA protein (Phizicky and Roberts, 1981), which is the repressor of RecA and the SOS response. The SOS response (Little and Mount, 1982; Walker, 1985) is mounted by *E. coli* cells after extensive DNA damage, and involves the induction of more than 17 genes, one of which is the RecA gene. With these assays, it is found that the active form of the RecA molecule is a polymeric complex containing the RecA protein, a polynucleotide substrate, and a nucleoside triphosphate cofactor. This complex is helical, with ~6.18 RecA subunits per 95Å pitch turn (DiCapua et al., 1982; Egelman and Stasiak, 1988). The RecA ATPase activity occurs throughout the helical filaments (Brenner et al., 1987), and this means that filaments formed in the presence of ATP are dynamic, with an ATPase turnover of about 30/min (Cox and Lehman, 1987). Previous structural studies of the RecA filament have therefore either depended upon fixation (Flory et al., 1984; Stasiak et al., 1984) or employed the relatively nonhydrolyzable ATP analogue, ATP-γ-S, as a nucleoside triphosphate cofactor (DiCapua et al., 1982; Egelman and Stasiak, 1986; Egelman and Stasiak, 1988). In the presence of ATP-γ-S, however, individual RecA filaments are still characterized by a large degree of disorder, due to the small flexural rigidity, the variations in the pitch of the helix, and the variations in the twist of the helix (Egelman and Stasiak, 1986; Egelman and Stasiak, 1988).

We report in this paper that a significant improvement in the helical order of RecA filaments can be obtained by inhibiting the RecA ATPase with aluminum fluoride. The more ordered RecA filaments yield details about RecA structure which were not previously obtainable. These observations were motivated by two recent results. Firstly, we have found that ATP-γ-S is hydrolyzed at a rate great enough (~1/30 min) to account for some significant component of the large helical disorder seen in RecA filaments in the electron microscope (Yu, X., and E. H. Egelman, manuscript in preparation). It appeared likely, therefore, that conditions which would completely inhibit the RecA ATPase would lead to an improvement in helical order. Secondly, Moreau and Carlier (1989) have shown that aluminum fluoride inhibits the RecA ATPase. They have reported that the complex of RecA-ADP-AlF_4^- is active in cleaving the LexA protein, suggesting both that AlF_4^- acts as a structural analogue for P_i, and that the release of products is the key step in the RecA ATPase cycle which allows the RecA protein to switch to an inactive state.

Dr. Yu's and Dr. Egelman's present address is Dept. of Cell Biology and Neuroanatomy, University of Minnesota Medical School, Minneapolis, MN 55455.

0006-3495/90/03/555/12 $2.00

MATERIALS AND METHODS

RecA and DNA preparation

RecA was purified by the method of West et al. (1982), with an additional polyspermidine precipitation, as described by Griffith and Shores (1985). The purified RecA ran as a single band on an SDS-PAGE Coomassie blue–stained gel.

Double-stranded, circular ϕX174 was a gift from Dr. Paul Howard-Flanders. The DNA was linearized by restriction endonuclease Pst-I (IBI), and ran as a single band on an agarose gel. The concentration of the DNA was measured using an extinction coefficient A_{260} of 1 for 50 μg/ml and a 1-cm pathlength.

Reactions of RecA and DNA were carried out at 37°C in 25 mM triethanolamine-HCl buffer (pH 7.2). RecA concentration was 7 μM. The RecA:double-stranded DNA ratio was equal to 40:1 (wt:wt) or a 1:3 molar ratio of RecA to total nucleotides. This is a twofold excess of RecA, given that each RecA protomer binds three base pairs or six nucleotides. ATP (Sigma Chemical Co., St. Louis, MO) concentration was 2.5 mM. Aluminum nitrate and sodium fluoride (both from J. T. Baker Chemical Co., Phillipsburg, NJ) were added to 2.5 mM.

Electron microscopy

Samples were prepared on carbon-coated copper grids which had been glow discharged. After a sample was placed on the grid, excess solution was removed by blotting with filter paper. Then the samples were negatively stained with 2% uranyl acetate and viewed with a Zeiss 10C electron microscope under an accelerating voltage of 80 kV. The magnification was calibrated with tobacco mosaic virus particles, using the 23-Å pitch of the right-handed one-start helix as a standard.

Image analysis

Electron micrographs were scanned with a model 78/99 digital camera (Eikonix Corp., Bedford, MA) interfaced to a VAX 3200 computer (Digital Equipment Co., Maynard, MA). Fourier transforms and other computations were accelerated with a Warrior array processor (Sky Computers, Chelmsford, MA). The procedures used in the analysis of filaments are as described in Egelman and Stasiak (1986, 1988).

The standard error of the mean at each pixel in an averaged map is:

$$\mathrm{SEM}_{i,j} = \frac{\left[\sum_{k=1}^{n} (\rho_{i,j}{}^{k})^2 - \left(\sum_{k=1}^{n} \rho_{i,j}^{k}\right)^2\right]^{1/2}}{[(n-1)n]^{1/2}},$$

where ρ_{ij}^{k} is the density at point i,j in the kth map. The standard error at every point in a difference map is then: $\sigma_{i,j}^{dif} = [(\mathrm{SEM}_{i,j}^{1})^2 + (\mathrm{SEM}_{i,j}^{2})^2]^{1/2}$. The densities in the difference map of Fig. 11 are divided by the standard error at every point in the difference map to show the significance of features.

RESULTS

Moreau and Carlier (1989) have shown that the complex of RecA-DNA-ADP-AlF_4^- is active in cleaving the LexA repressor molecule. We have used electron microscopy to examine the form of this complex. An initial reaction mixture of RecA (7 μM), double-stranded DNA (21 μM in nucleotides), and ATP (2.5 mM) was incubated at 37°C for 5 min. Aluminum nitrate (2.5 mM) and sodium fluoride (2.5 mM) were then added and further incubated at 37°C for 15 min. Electron micrographs taken after this time displayed the characteristic 95-Å pitch filaments (Fig. 1) that look indistinguishable from those prepared with ATP-γ-S or ATP (Egelman and Stasiak, 1986). A control experiment was performed where aluminum nitrate and sodium fluoride were not added, and the RecA was incubated with DNA and ATP for a total time of 20 min. No filaments were observed in the electron microscope, because the ATP pool would be almost completely hydrolyzed by the RecA under these conditions.

We have found that the initial incubation with ATP alone is essential for filament formation to occur. When ATP (2.5 mM), aluminum nitrate (2.5 mM), and sodium fluoride (2.5 mM) were added together initially, no filaments were observed after a 20-min incubation. Similarly, when ADP (2.5 mM), aluminum nitrate (2.5 mM), and sodium fluoride (2.5 mM) were added together initially, no filaments were observed after a 20-min incubation.

Approximately 50 images of filament sections were scanned, corrected for curvature (Egelman, 1986), and Fourier transformed. The mean length for the sections used was 2,178 Å, with the minimum length of 1,560 Å and a maximum length of 2,838 Å. From these filament sections, 35 were found which displayed useable Fourier transforms. Such Fourier transforms (Fig. 2) of these RecA-DNA-ADP-AlF_4^- filament segments showed that these filaments display greater helical order than filaments which have been prepared with ATP-γ-S (Egelman and Stasiak, 1986). Whereas most filaments formed with ATP-γ-S will display a strong layer line (n = 1) arising from the right-handed 95-Å pitch helix and some will display a weak second order (n = 2) of this layer line, filaments formed with AlF_4^- consistently display a second order layer line that is stronger than that seen with ATP-γ-S. One filament was found with a third order (n = 3, at 1/31 Å). More importantly, 16 filaments were found which displayed a symmetrical layer line slightly above the prominent 1/95 Å layer line at a spacing of ~1/81 Å. Among these filaments, a number displayed symmetrical layer lines at spacings of ~1/570, 1/114, 1/52, and 1/44 Å. In all cases, however, the 1/95 Å layer line dominates the transform, with an intensity that is usually over 10 times greater than that of any other layer line.

The indexing of these layer lines was straightforward. The strongest layer line, 1 = 6, arises from the 95-Å pitch right-handed helix, and contains a Bessel order n = 1. Examination of the 1/81-Å layer line showed a 180° phase difference between the near and far sides, indicating that this layer line contains an odd Bessel order. The

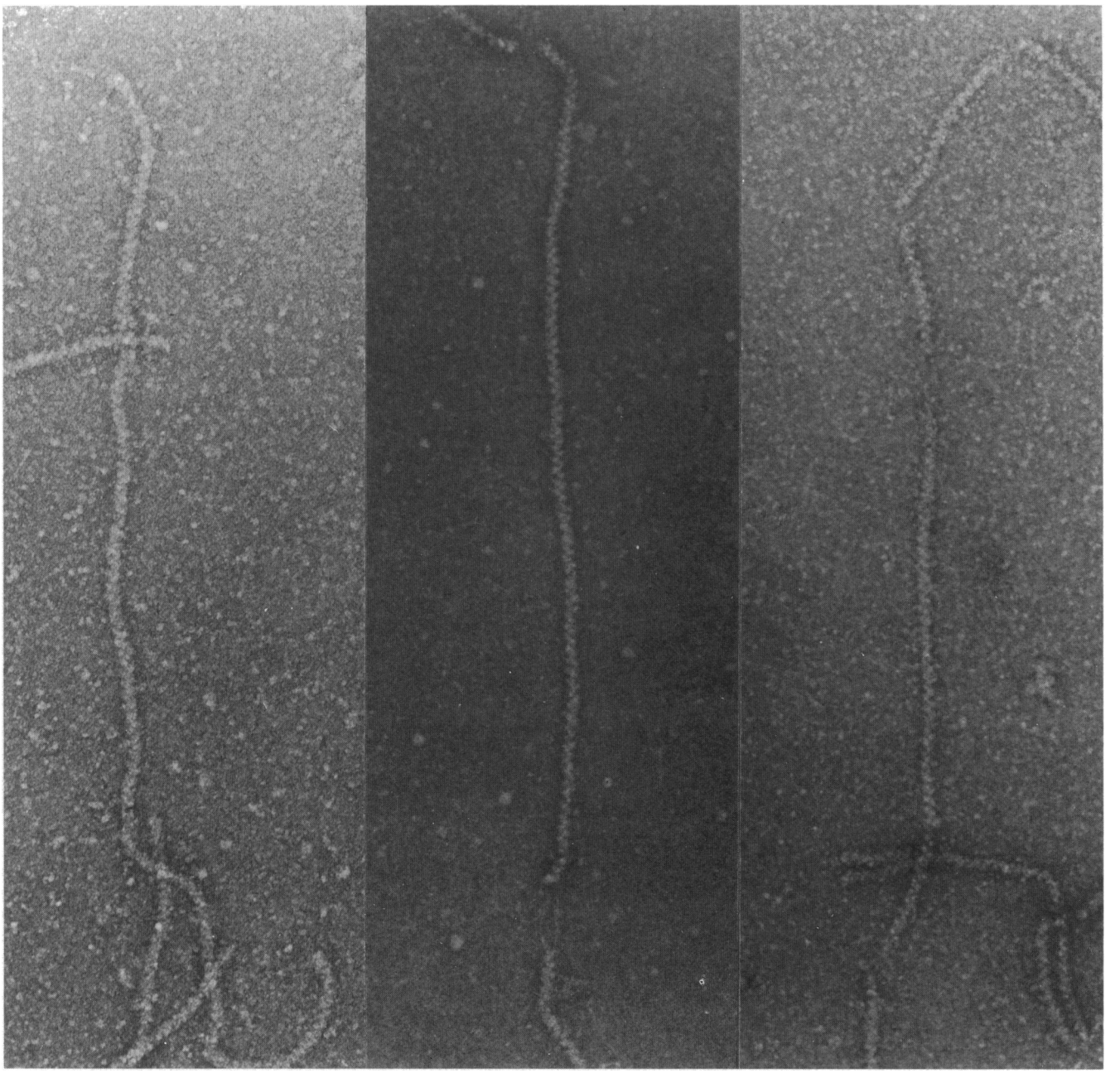

FIGURE 1 Electron micrographs of negatively stained RecA filaments formed on linear double-stranded DNA in the presence of ATP and aluminum fluoride. The aluminum fluoride substitutes for phosphate after the hydrolysis of the ATP, and the complex of RecA-ADP-AlF_4^- is stable over time. The electron micrographs were prepared after a 5-min incubation with ATP, followed by an additional 15-min incubation with the aluminum fluoride. In a control experiment, where no aluminum fluoride is added, no filaments are found, as the ATP pool has been completely hydrolyzed. The mean pitch of the filaments is ~92 Å, and the filaments are ~100 Å wide.

peak on this layer line occurs at a radial spacing of ~0.020 $Å^{-1}$. Because the filaments are ~100 Å in diameter, this could arise from a Bessel order 5 where contrast is generated at an outer radius, or a Bessel order 3 generated at a smaller radius. Higher Bessel orders are excluded. Examination of the phases on other layer lines showed that the first is even, the fifth is odd, and the 13th is even. Because the peak on the fifth layer line occurs at a higher radius than the peak on the seventh layer line, the first and seventh layer lines most likely contain negative Bessel

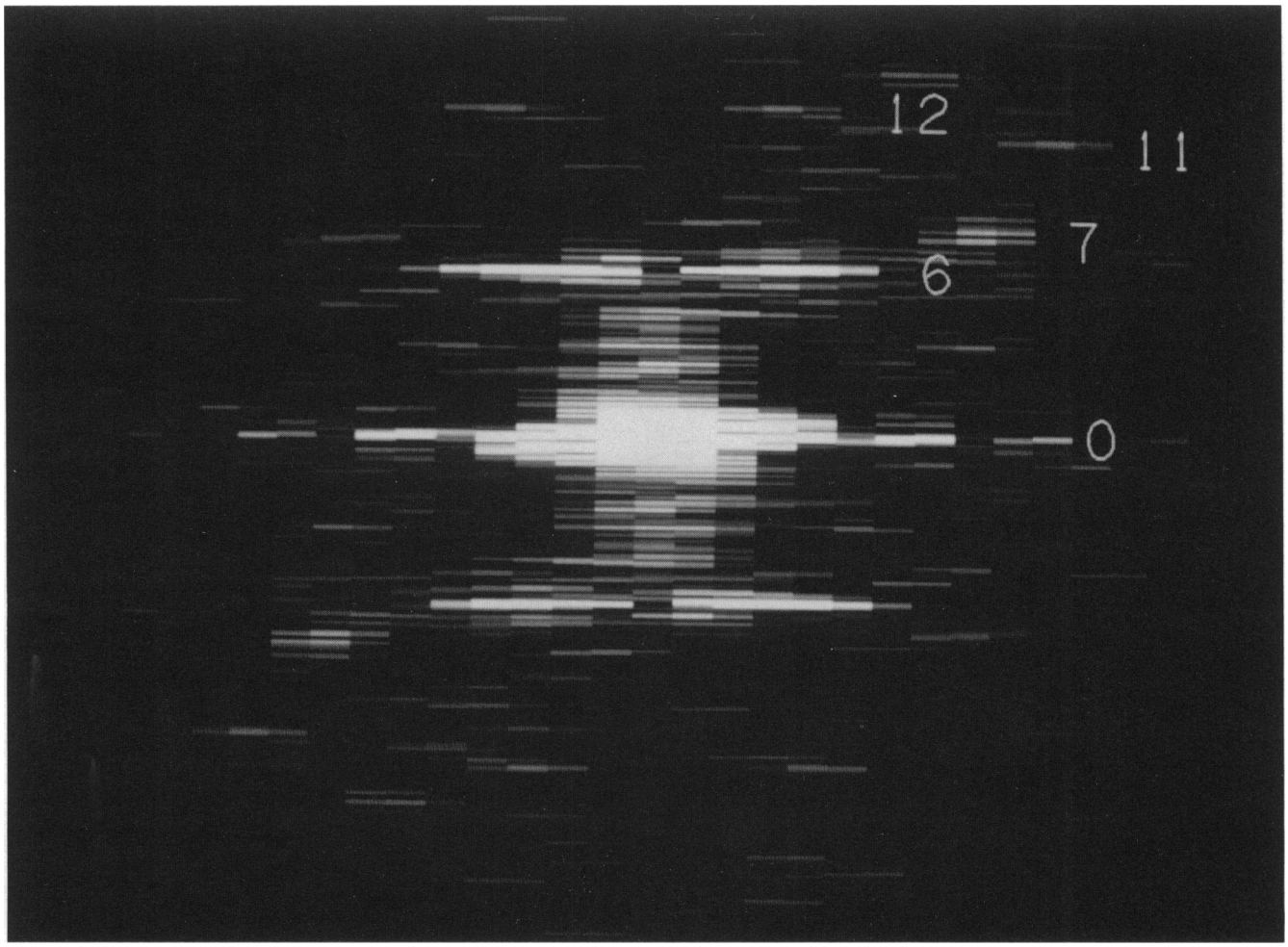

FIGURE 2 A 128 × 2,048 point computed Fourier transform of a RecA-DNA-ADP-AlF_4^- filament. The strongest layer line, 6, is at a spacing of ~1/95 Å. Although almost all of the 40 filaments which were examined showed a 12th layer line, 16 filaments were selected which showed a strong and symmetrical seventh layer line. A few individual filaments can be seen with an 11th layer line, as shown here, and other filaments can be seen with a 1st, 5th, 13th, and 18th layer line. Although the spacing of the sixth layer line in this particular transform is ~5.1 times the distance between the sixth and seventh layer line and the 11th and 12th layer line, the layer lines are indexed as arising from a 37/6 helix for every filament because the average of the population is close to that value.

orders, corresponding to left-handed helices. The most reasonable indexing scheme is given in the n,1 plot in Fig. 3.

If the indexing of Fig. 3 is correct, one can use the layer line spacings to determine the number of units/turn of each individual filament. The data shown in Fig. 4 yields a mean of 6.1743, with a standard error of the mean of 0.005. This value is in excellent agreement with the symmetry of RecA filaments determined by other means. From a knowledge of the number of base pairs in a closed circular double-stranded DNA molecule, the number of RecA striations, and the binding stoichiometry, DiCapua et al. (1982) were able to determine that there are 6.18 ± 0.016 (our estimate of the error) RecA subunits per turn of the helix in the ATP-γ-S state. Observations of three-filament and six-filament bundles of RecA has shown that the symmetry of the component filaments is about 6.152 ± .004 units per turn in these structures (Egelman and Stasiak, 1988). Different indexing schemes from the one shown in Fig. 3 would yield very different values for the twist of the filaments. For example, if layer line 7 was $n = -3$, the symmetry would be ~4.17 units per turn. Thus, prior knowledge of the approximate twist of the filaments can be used to establish that the indexing of Fig. 3 is indeed correct.

An interesting feature of the data shown in Fig. 4 is that there is a significant correlation between the twist and the pitch of the 16 filaments examined. As filaments

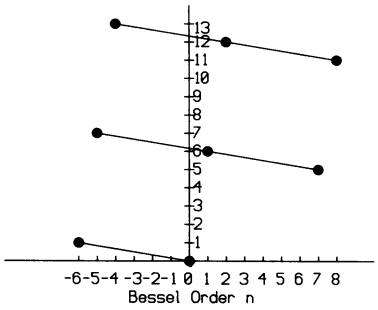

FIGURE 3 The n,1 plot for the transform of Fig. 2. Dots indicate the allowed Bessel orders for layer lines 0, 1, 5, 6, 7, 11, 12, and 13. These Bessel orders are determined by the selection rule for a helix with 37 subunits in six turns.

are extended, they untwist (the number of units per turn increases, so the angular increment between subunits decreases). This is the same form of mechanical coupling that we have described for bundles of six RecA filaments formed with 10 mM Mg^{2+} (Egelman and Stasiak, 1988). This data may also be used to describe the mechanical linkage within the DNA in the filaments, because it has been shown topologically that DNA has the RecA helical twist imposed upon it (Stasiak and DiCapua, 1982). When DNA goes from the B-form, with 3.4 Å rise per base pair, to the stretched form in the complex with RecA (5.1 Å rise per base pair), it is untwisted from 10.5 units per turn to ~18.6 units per turn. Because there are three base pairs per RecA subunit, the data in Fig. 4 may be expressed in base pairs per turn, ranging from 18.42 to 18.62 base pairs per turn. The linear regression line which is drawn has the same positive slope as the line which would extrapolate from the center of this distribution to the point for B-DNA (10.5 base pairs per turn, 35.7 Å pitch), but has about three times the magnitude.

Layer line data was combined from the 16 filaments and used to produce an averaged layer line set (Fig. 5). The method which was used involved choosing one filament as an initial reference and fitting all other filaments to this reference. An average was created, which was then used as a new reference. This was repeated for several cycles, but converged completely after only two iterations. One filament was subsequently dropped from this average due to poor agreement with the rest, and has not been included in the data shown. The statistics of averaging can be seen in Fig. 6, where the amplitude-weighted phase residuals are shown for each filament data set against the average data.

Three-dimensional reconstruction

A three-dimensional reconstruction was computed from the averaged layer line data, and sections cut perpendicu-

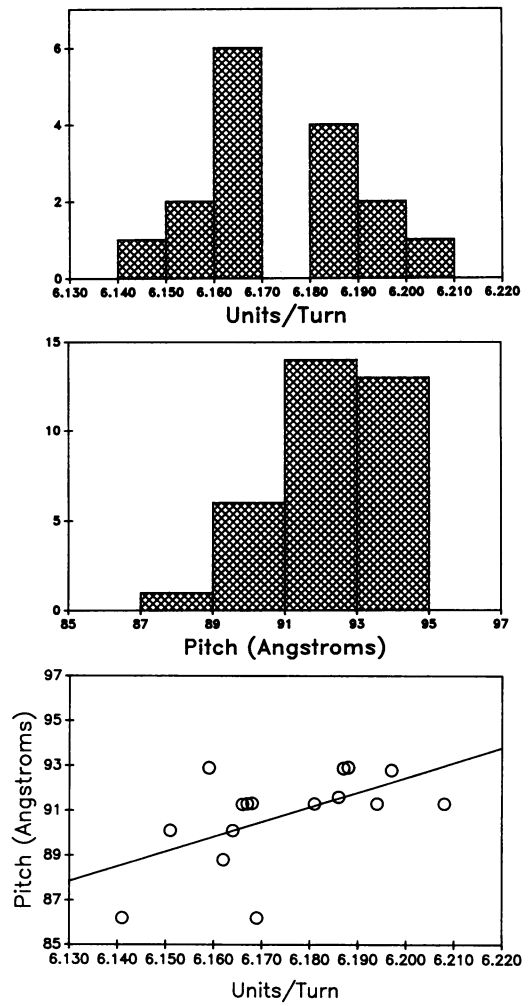

FIGURE 4 The actual spacing of layer lines in the transform of filaments can be used to accurately determine the twist of the filaments (in units per turn of the helix) (*A*). Because the twist is given by a ratio of layer line spacings, it is independent of magnification. From the indexing of the transform, the number of units per turn will be equal to $6 + Z_1/Z_6$, where Z_1 and Z_6 are the axial spacings of the first and sixth layer lines, respectively. The value used for Z_1 was actually $Z_7 - Z_6$. For the set of 16 filaments which gave a well-defined and symmetrical seventh layer line, the mean number of units per turn is 6.1743, with a standard error of the mean of 0.005. The pitch has been determined by measuring the spacing of the sixth layer line, nominally at 1/95 Å, using the 1/23 Å layer line of coprepared tobacco mosaic viruses as a magnification standard (*B*). A significant correlation exists between the twist and the pitch. The coefficient of correlation is $r = 0.567$, with a standard error of 0.1328. From Student's t test, the probability that this sample is from a population with no correlation is <0.001. Linear regression line to the data is shown. As filaments are extended (the pitch increases) the filaments untwist (the number of units per turn increases).

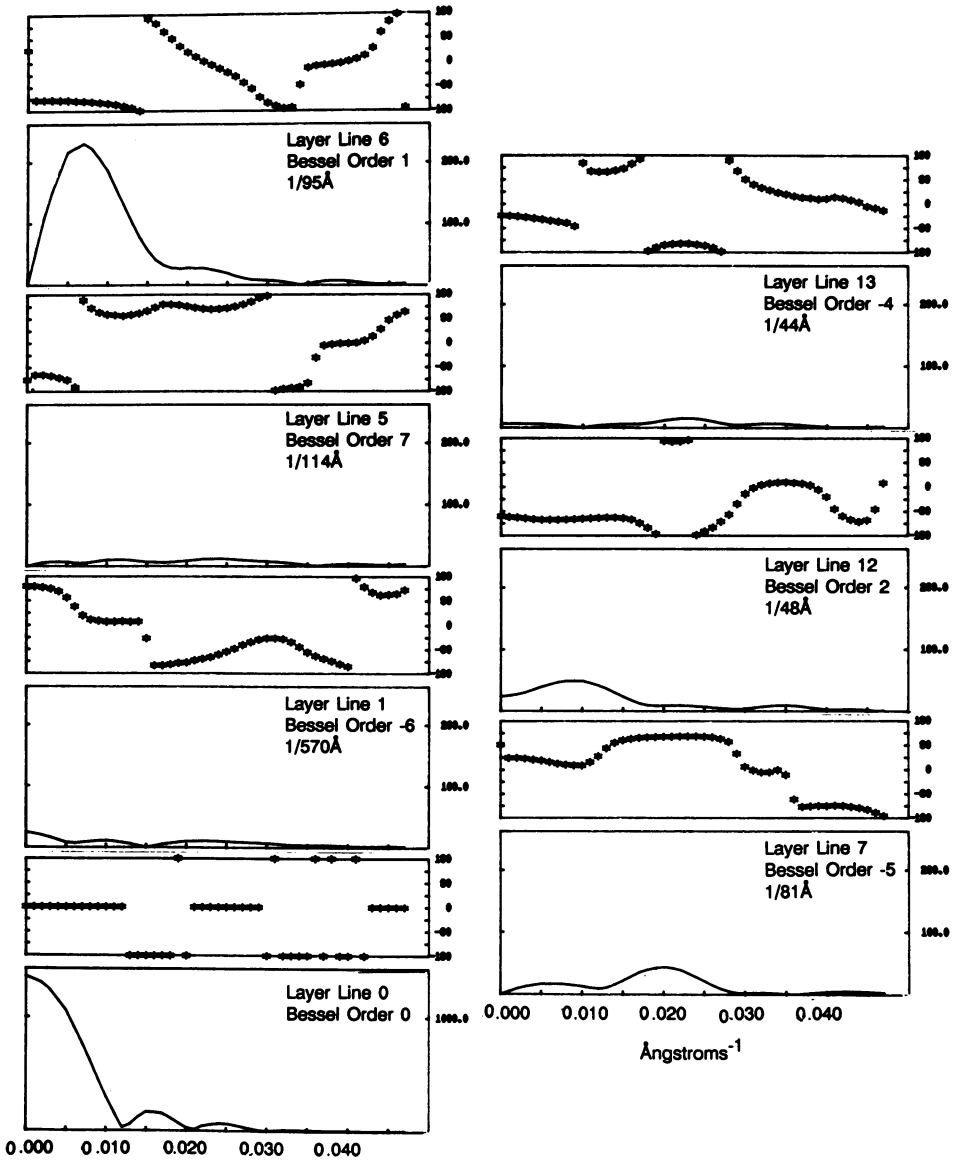

FIGURE 5 Amplitudes and phases for the averaged set of seven layer lines from 15 filaments. Each individual filament was first averaged with respect to the near and far sides before it was averaged with the other filaments. The amplitude scale is the same for all the layer lines except the equator.

lar to the filament axis are shown in Fig. 7. The outer contour was chosen such that the correct molecular volume is enclosed, using the RecA molecular weight of 38 k and a volume of 1.2 Å^3/k, corresponding to a partial specific volume of 0.75 cm^3/g. The asymmetric unit in the helix is visualized as two distinct domains, most clearly seen in the section at $z = 0$ Å in Fig. 7. When sections are stacked, it can be seen that one subunit extends axially for ~45 Å, or almost half of one helical turn. Although subunits cannot be unambiguously and uniquely cut out of the filament density in the absence of the ability to trace the polypeptide chain, the general boundaries associated with the subunit appear suggestive, and these have been outlined in Fig. 7.

Surface views of the reconstruction are shown in Fig. 8. One loses all details of the internal structure in this rendering, and no information about the two-domain structure is conveyed.

Analysis of the error

The confidence with which one can assess features in the map can be determined quantitatively by an estimation of the variance which occurs at every point in the density of

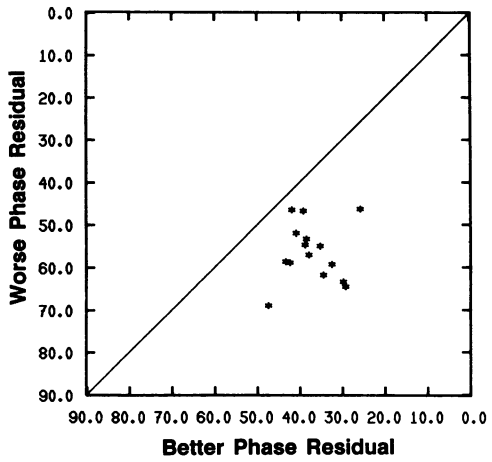

FIGURE 6 The total amplitude weighted phase residual between each of the 15 layer line sets used in the average and the averaged layer line set itself (Fig. 5), as a function of the polarity of each individual set against the averaged data set. This plot can serve as a measure of the intrinsic polarity of the structure. For a nonpolar structure (or for highly noisy data) there would be no significant difference between the two different orientations of each individual data set, and all points would fall near the diagonal line. The further points are from the diagonal, the greater the measure of polarity. The centroid of the distribution is 37° for the better phase residual, and 58° for the opposite orientations.

the averaged map. Fig. 9 shows the standard error of the mean at every pixel within three sections of the averaged map. It can be seen that the main peaks of the variation fall on the inner domain of the RecA subunit, but that these peaks are relatively small compared to the actual map densities. While the peaks within the domains are >53 density units, the largest standard error is only ~3.3 density units. Within most of the map, the standard error of the mean is less than the spacing between successive contour lines. Thus, the features which are shown by the contours are quite reliable.

A different method of assessing the reliability of the visualization of two domains was provided by randomly dividing the data set into two groups, one of eight filaments and the other of seven filaments, and independently averaging and reconstructing these sets. The resulting maps are shown in Fig. 10, where two domains can be seen in each of the independent maps. The inner domain of map A is weaker than that of map B, and this is consistent with the peak of the variance in Fig. 9 lying on this feature. The origin of this variance is not yet known, and could arise from either variations in the pattern of stain penetration or actual variations in the structure of the protein.

Comparison with the ATP-γ-S state

The general characteristics of filaments formed with AlF_4^- appear indistinguishable from those of filaments formed with ATP-γ-S. The mean pitch of 35 filaments (the sample from which the 15 filaments were taken) formed with AlF_4^- was 92.1 Å, with an SEM of 0.3 Å, whereas a corresponding sample of 39 filaments formed with ATP-γ-S on dsDNA (Egelman and Yu, 1989) had a mean pitch of 92.3 Å with an SEM of 0.3 Å. The helically averaged cross-sections from both of these samples are shown in Fig. 11. It should be noted, however, that the subsample of 16 AlF_4^- filaments used for the data in Fig. 4 had a mean pitch of 90.8 ± 0.5 Å (SEM), and thus appear to be shifted to a smaller pitch from the parent sample. The twist of individual filaments in the ATP-γ-S state cannot be compared with the twist in the AlF_4^- state (because, in general, it cannot be determined in the ATP-γ-S state), but the mean twist of the AlF_4^- filaments (6.174 ± 0.005 units per turn) is quite close to what has been determined for bundles of RecA filaments (see above).

The averaged reconstruction of the RecA-dsDNA-AlF_4^- filament may be compared with the reconstruction of a single RecA-dsDNA-ATP-γ-S filament (Egelman and Stasiak, 1986). That reconstruction was computed from a filament section which came from one extremum

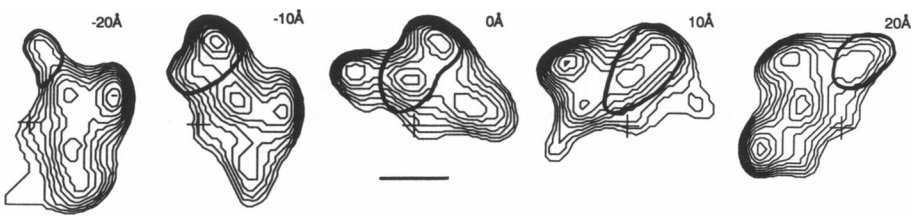

FIGURE 7 The layer line set of Fig. 5 has been used to compute a three-dimensional reconstruction of the RecA filament. Sections which have been cut perpendicular to the filament axis are shown at spacings of 10 Å. Filament axis is indicated in each section by the cross. An individual RecA subunit (38 k mol wt) extends axially for ~45 Å, and one particular subunit is delineated by the thick boundary which is drawn on each section. Two clear domains in the RecA subunit are seen in the axial section which cuts through the middle of the indicated subunit, labeled as $z = 0$ Å. The outer contour has been chosen to yield the correct molecular volume. Scale bar, 39 Å.

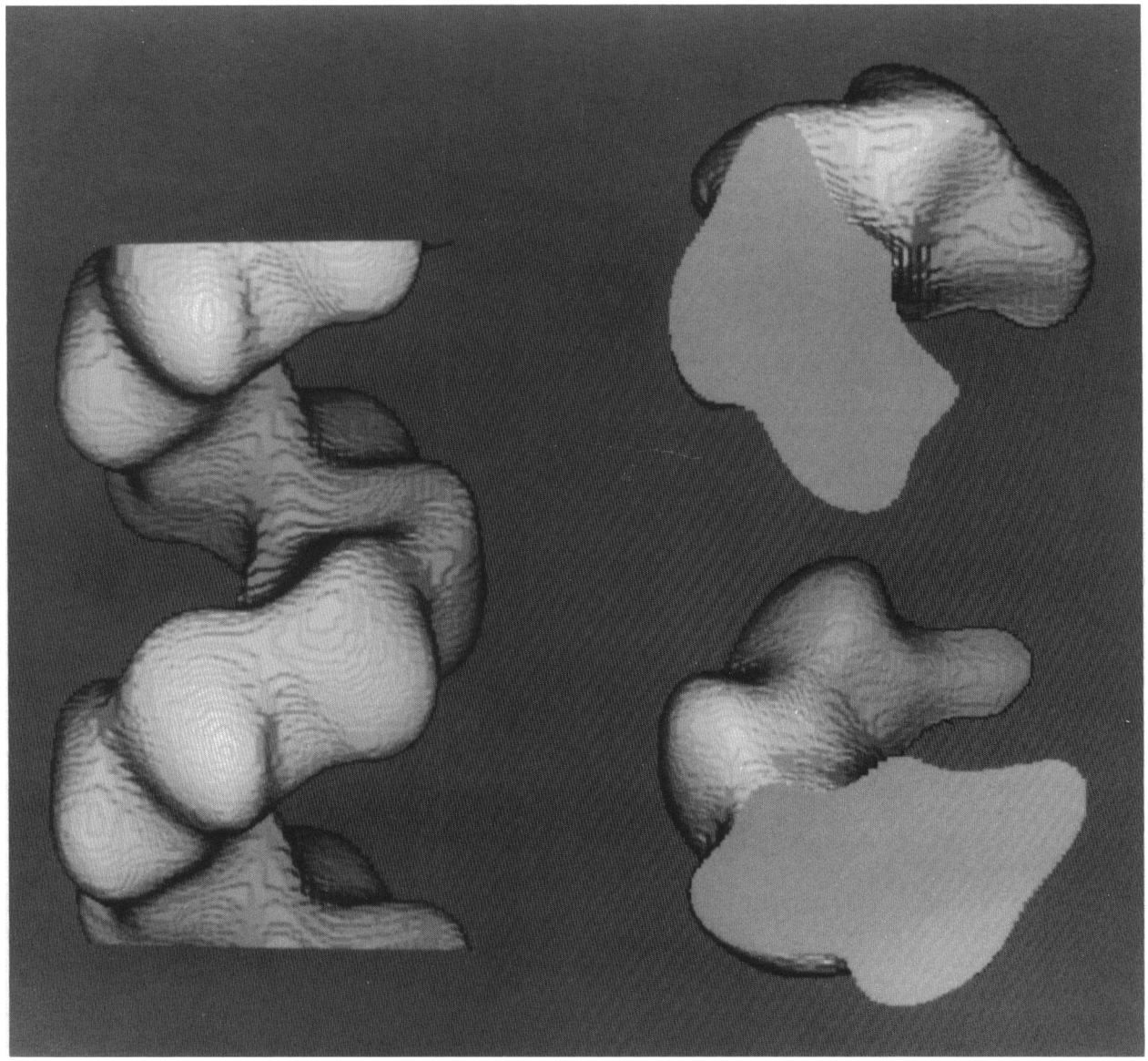

FIGURE 8 The surface of the reconstruction shown in Fig. 7 is shown in a side view (*left*), and in 40-Å-thick sections cut perpendicular to the filament axis (*right*). From previous work (Stasiak et al., 1988), we know that the 3′ end of a single-stranded DNA would be at the bottom, and the 5′ end would be at the top. The view on the top is from the 5′ end towards the 3′ end, while the view at the bottom is from 3′ to 5′.

of the data, with ~100 Å pitch and 5.1 units per turn. The general features of the filament density appear very similar, but it is difficult to determine whether the differences which exist arise from the fact that the single ATP-γ-S filament which was used was at an extremum, whether the data itself was noisy, or whether there are small structural differences between the state formed with ATP-γ-S and that formed with AlF_4^-. If that ATP-γ-S filament came from the same population as the AlF_4^- filaments, the data of Fig. 4 suggests that the filament should have ~6.3 units per turn based upon its pitch, rather than the 5.1 units per turn observed. This may mean that the structural state is different, or at least that the relationship between pitch and twist is different with ATP-γ-S. An analysis of the variance in the present reconstruction (see above) suggests that the features seen in the 1986 reconstruction are within the range of variation seen within the present data set. A more direct quantitative comparison between reconstructions of filaments formed with AlF_4^- and filaments formed with ATP-γ-S is not possible, due to the fact that we have data on only one filament in the ATP-γ-S state. That is, we

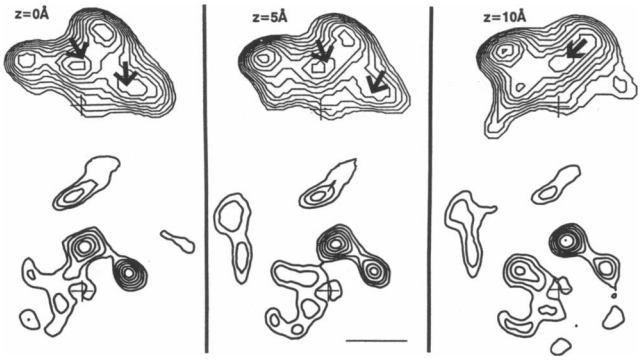

FIGURE 9 The standard error of the mean-averaged density at every point in the averaged map is shown for three different cross-sections, at z = 0, 5, and 10 Å. Scale bar under the z = 5 Å section is 30 Å. Because the axial rise per subunit is ~15.4 Å, and the rotation between subunits is 360°/(37/6), the section at z = 15 Å will be almost identical with the section at z = 0 Å, but rotated by 58.4°. The contouring steps for the sections and the SEMs are very different. The sections have been contoured in steps of 1.5 arbitrary density units, starting at ~37, with a peak density of ~55 units. The SEMs have been contoured in steps of 0.25 density units, starting at 2.0, with a peak of ~3.3. Thus, the largest single SEM is just slightly more than the spacing of two contours, while the error in most of the map is about the spacing of one contour line. The arrows indicate where the largest peaks in the variance fall on the density maps themselves. It can be seen that the major peaks fall on the inner domains.

have an estimate of the variance present in AlF_4^- filaments, but an assumption of homoscedasticity (that the variance is the same for both populations) is almost certainly wrong given the increased disorder present in the ATP-γ-S state. However, one can directly compare the helical projections from each of these states, computed with the equator, the n = 1 (1/95 Å) and the n = 2 (1/47.5 Å) layer lines. Such a comparison is shown in Fig.

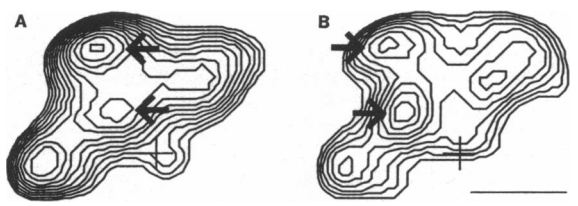

FIGURE 10 A different assessment of the confidence with which one can see two domains in the RecA subunit was provided by randomly dividing the data set into two groups, one of eight filaments and the other of seven filaments. These groups were averaged together independently using the iterative procedure described. A single section of the map generated from the seven filaments is in *A*, and the corresponding section of the map from the remaining eight filaments is in *B*. The scale bar is 30 Å, and the crosses mark the location of the filament axis in each panel. The arrows point to the two domains which are visualized in each of these subsets.

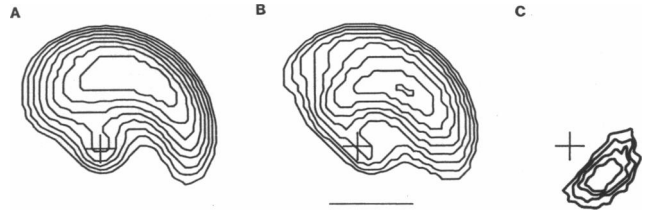

FIGURE 11 Helical projections are compared between RecA-dsDNA-ATP-γ-S filaments (*A*) and RecA-dsDNA-AlF_4^- filaments (*B*). An average of 39 filaments was used for *A* (Egelman and Yu, 1989), whereas 35 filaments were used for *B*. The helical projections were computed with the equator, the n = 1 (1/95 Å) and the n = 2 (1/47.5 Å) layer lines. The difference map (AlF_4^--ATP-γ-S) (*C*) has been divided by the standard error of the difference at every point in the map, and is contoured in levels of standard deviations, with the lowest contour at 2.5 and the peak at 4 standard deviations. The differences are positive, indicating that the densities in the AlF_4^- map are higher in this region. Scale bar under *B* is 30 Å, and crosses mark the position of the helix axis in each of the panels.

11, where one may see that there is only one region of statistically significant difference between the two projections, and that this occurs on the edge of the filament density. Such a difference could be due to the motions of subunit density at the periphery from disorder, or could be due to a small conformational difference between the two states.

In the light of recent results, it is possible to reinterpret the 1986 ATP-γ-S reconstruction. A continuous column of density was present there at ~16 Å radius which followed the right-handed one-start helix. This feature was interpreted as one possible location for the DNA in Fig. 18 *a* of Egelman and Stasiak (1986), assuming that the DNA stained negatively in the complex. A different possibility was also presented for the possibility that the DNA stained positively. We now know that the DNA does indeed stain negatively, but that it is almost on the axis of the complex (Egelman and Yu, 1989). Thus, a possibility to be considered is that the column of density at 16 Å radius was actually the inner domain of RecA which was not resolved into discrete subunits as it is in the present paper. The failure to resolve the inner domain in the previous reconstruction is also consistent with our observation in the present work that most of the variance falls on the inner domain (see Fig. 9).

DISCUSSION

Moreau and Carlier (1989), on the basis of an assay involving RecA cleavage of the LexA protein, concluded that the RecA-ADP-AlF_4^- state is a stable analogue of the RecA-ADP-P_i state, and that this state has the same activity as the RecA-ATP state. We have shown structur-

ally that with the exception of the increased order, the RecA-ADP-AlF_4^- filaments appear very similar to those formed with ATP-γ-S, and presumably, ATP. Of course, the comparison is limited by the available resolution and the greater disorder present in the ATP-γ-S state. Given that the AlF_4^- state is an analogue for the ADP-P_i state, at some level the conformation of this state must differ from the ATP state, because the energy of the phosphate bond which has been cleaved will most likely be stored in an "activated" state of the protein. The "activated" state of the protein will subsequently undergo a major conformational change associated with the release of the products. Thus, it is possible that the difference seen in Fig. 11 between the helically averaged AlF_4^- and ATP-γ-S densities could be due to such a small conformational change. More information is clearly needed.

The increased order present in RecA-ADP-AlF_4^- filaments compared with RecA-ATP-γ-S filaments suggest that AlF_4^- inhibits the RecA ATPase to a greater extent than ATP-γ-S. It is also consistent with our observations that ATP-γ-S is hydrolyzed at a rate which is significant for structural studies (Yu, X., and E. H. Egelman, manuscript in preparation). The hydrolysis of ATP-γ-S yields a mixture of biochemical states in the filament images: some subunits may have a bound ATP-γ-S, some may have a bound ADP, some may have no bound

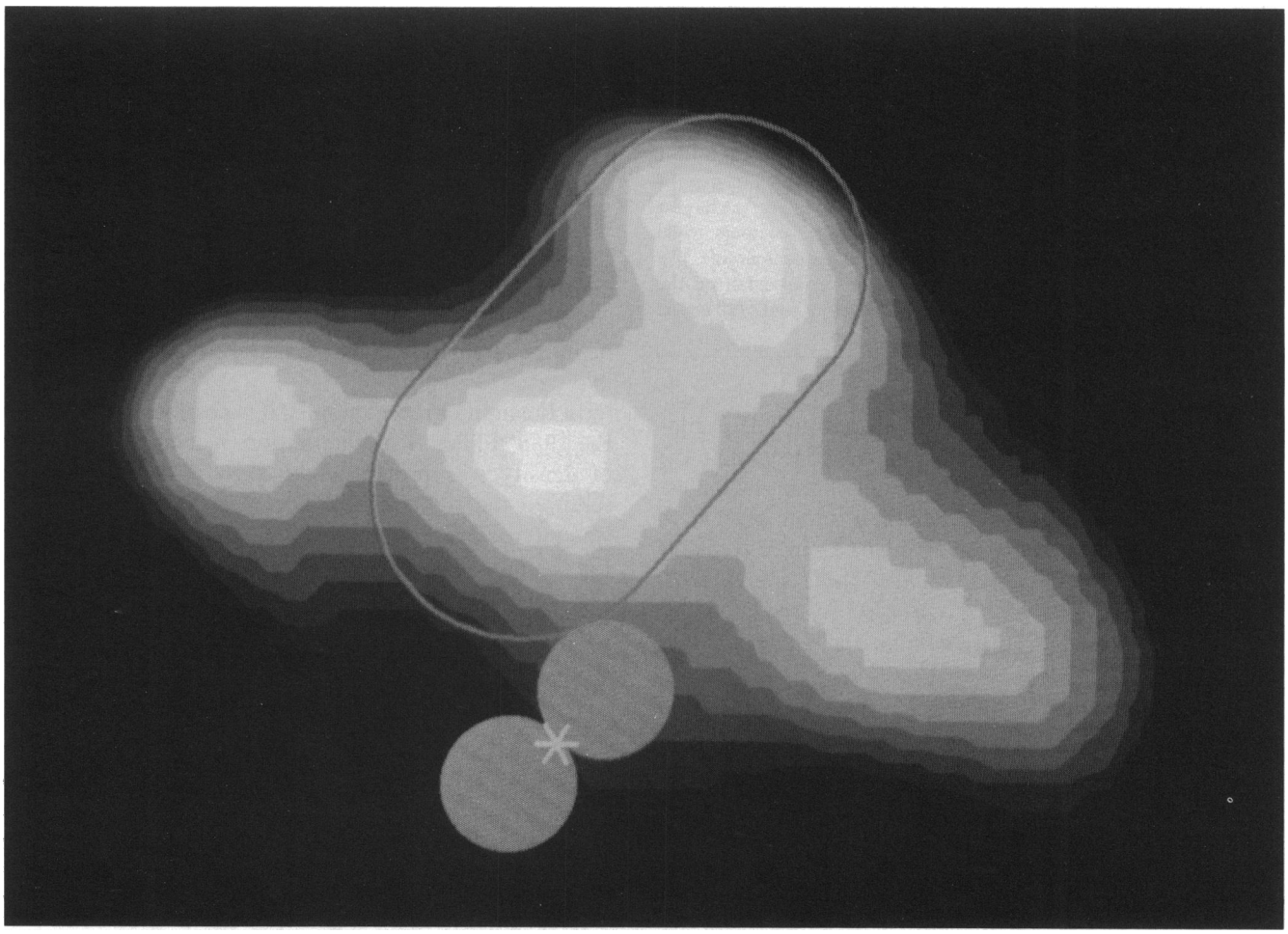

FIGURE 12 The position of the DNA in the RecA-DNA filament has been determined by generating a difference map between RecA filaments formed on double-stranded DNA and RecA filaments formed on single stranded DNA (Egelman and Yu, 1989). The cross-section which is shown is that of $z = 0$ Å in Fig. 7, with one subunit roughly outlined. The filament axis is shown by the star; two strands of DNA around the axis are labeled 1 and 2. Strand 1 has been directly visualized (Egelman and Yu, 1989), and is one strand of a double-stranded DNA. The position of strand 1 has been determined by aligning the helical projection of Egelman and Yu (1989) with a helical projection of the AlF_4^- state (Fig. 11 *b*). The other strand of double-stranded DNA binds to RecA in the same place as a strand of single-stranded DNA, and thus does not appear in a difference map. This strand has been arbitrarily placed at position 2 in this figure. However, given that this strand must be in contact with the protein, and given that it must be the same distance from the helical axis for the two strands to be symmetrical, there is a rather limited range of positions in which this strand can be located.

cofactor, and others will have the bound products before release.

RecA clearly undergoes large conformational changes, but they are associated not with the hydrolysis of the nucleotide cofactor, but with the release of the products. RecA filaments formed in the presence of ADP or in the absence of nucleotide cofactors are characterized by a 65 Å pitch (Stasiak and Egelman, 1986), and it may be imagined that the hydrolysis of ATP or ATP-γ-S and the release of the products leads to local compressional motions within a filament that is basically in an extended state. However, an analysis of conformational changes associated with the hydrolysis of ATP-γ-S seen in bundles of RecA filaments (Egelman and Stasiak, 1988; Egelman, E. H., and X. Yu, manuscript in preparation) shows that these motions and conformational changes are largely rotational. Thus, the filaments formed with ADP may be an in vitro artefact and irrelevant to understanding RecA function.

RecA organized into two domains

The most significant feature of the RecA filament reconstruction is the visualization of two domains within the RecA protomer. A previous biochemical study, using trypsin digestion, concluded from the pattern of cleavage of the RecA protein that it is organized into two nearly equal structural domains (Kobayashi et al., 1987). The direct visualization of DNA within the RecA-DNA filament (Egelman and Yu, 1989) has now given us a greater ability to relate RecA structural organization to function. The information on DNA position has been combined with the present data in Fig. 12, where one can see that the DNA molecule which is covered by the RecA filament (as opposed to the second DNA molecule which must enter the complex to establish homologous contacts) is only in contact with the inner domain of the RecA subunit. It would be tempting to speculate that the outer domain contains a second DNA binding site obtained through a process of domain replication, but RecA–RecA sequence comparisons show no significant internal repeats within the primary amino acid sequence (data not shown). The main significance of the two-domain organization of the protein may involve dynamics. Kobayashi et al. (1987) showed that the pattern of proteolytic digestion of RecA was a function of the nucleotide cofactor, and suggested that nucleotide binding was responsible for a conformational change in the RecA protein. Another filamentous protein with an ATPase activity, actin, is also organized into two nearly equal structural domains (Suck et al., 1981), and the site of ATP binding in actin has been identified as being between the two domains. It is possible that the hydrolysis of ATP is associated with a large change in the domain–domain organization of the RecA subunit, and that this rearrangement is responsible for the rotation of subunit mass which is seen within bundles of RecA filaments (Egelman and Stasiak, 1988). A key question in understanding RecA-mediated recombination is explicating the relationship between such rotational motions and the transfer of a DNA strand from one DNA molecule to another. Studies are in progress to directly relate the motions of RecA associated with the hydrolysis of the nucleotide cofactor to the strand transfer activity.

This work was supported by National Institutes of Health grant GM35269 and National Science Foundation grant DMB 87-12075.

Received for publication 29 June 1989 and in final form 20 October 1989.

REFERENCES

Brenner, S. L., R. S. Mitchell, S. W. Morrical, S. K. Neuendorf, B. C. Schutte, and M. M. Cox. 1987. RecA protein-promoted ATP hydrolysis occurs throughout recA nucleoprotein filaments. *J. Biol. Chem.* 262:4011–4016.

Cox, M. M., and I. R. Lehman. 1987. Enzymes of general recombination. *Annu. Rev. Biochem.* 56:229–262.

DiCapua, E., A. Engel, A. Stasiak, and Th. Koller. 1982. Characterization of complexes between RecA protein and duplex DNA by electron microscopy. *J. Mol. Biol.* 157:87–103.

Egelman, E. H. 1986. An algorithm for straightening images of curved filaments. *Ultramicroscopy.* 19:367–374.

Egelman, E. H., and A. Stasiak. 1986. The structure of helical RecA-DNA complexes. I. Complexes formed in the presence of ATP-γ-S or ATP. *J. Mol. Biol.* 191:677–697.

Egelman, E. H., and A. Stasiak. 1988. Structure of helical RecA-DNA complexes. II. Local conformational changes visualized in bundles of RecA-ATP-γ-S filaments. *J. Mol. Biol.* 200:329–349.

Egelman, E. H., and X. Yu. 1989. The location of DNA in helical RecA-DNA filaments. *Science (Wash. DC).* 245:404–407.

Flory, J., S. S. Tsang, and K. Muniyappa. 1984. Isolation and visualization of active presynaptic filaments of RecA protein and single-stranded DNA. *Proc. Natl. Acad. Sci. USA.* 81:7026–7030.

Griffith, J., and C. G. Shores. 1985. RecA protein rapidly crystallizes in the presence of spermidine: a valuable step in its purification and physical characterization. *Biochemistry.* 24:158–162.

Howard-Flanders, P., S. C. West, and A. Stasiak. 1984. Role of RecA protein spiral filaments in genetic recombination. *Nature (Lond.).* 309:215–220.

Kobayashi, N., K. Knight, and K. McEntee. 1987. Evidence for nucleotide-mediated changes in the domain structure of the RecA protein of *E. coli. Biochemistry.* 26:6801–6810.

Little, J. W., and D. M. Mount. 1982. The SOS regulatory system of *Escherichia coli. Cell.* 29:11–22.

Moreau, P. L., and M.-F. Carlier. 1989. RecA protein-promoted cleavage of LexA repressor in the presence of ADP and structural analogues of inorganic phosphate, the fluoride complexes of aluminum and beryllium. *J. Biol. Chem.* 264:2302–2306.

Phizicky, E. M., and J. W. Roberts. 1981. Induction of SOS functions: regulation of proteolytic activity of *E. coli* RecA protein by interaction with DNA and nucleoside triphosphate. *Cell.* 25:259–267.

Stasiak, A., and E. DiCapua. 1982. The helicity of DNA in complexes with RecA protein. *Nature (Lond.)*. 299:185–186.

Stasiak, A., and E. H. Egelman. 1986. The structure and dynamics of recA protein: DNA complexes as determined by image analysis of electron micrographs. *Biophys. J.* 49:5–7.

Stasiak, A., A. Z. Stasiak, and T. Koller. 1984. Visualization of RecA-DNA complexes involved in consecutive stages of an in vitro strand exchange reaction. *Cold Spring Harbor Symp. Quant. Biol.* 49:561–570.

Suck, D., W. Kabsch, and H. G. Mannherz. 1981. Three dimensional structure of the complex of skeletal muscle actin and bovine pancreatic DNase I at 6 Å resolution. *Proc. Natl. Acad. Sci. USA.* 78:4319–4323.

Walker, G. C. 1985. Inducible DNA repair systems. *Annu. Rev. Biochem.* 54:425–457.

West, S. C., E. Cassuto, and P. Howard-Flanders. 1982. Postreplication repair in *E. coli:* strand exchange reactions of gapped DNA by RecA protein. *Mol.& Gen. Genet.* 187:209–217.